Optimization of the Immobilization Conditions of Horseradish Peroxidase on TiO₂-COOH nanoparticles by Box-Behnken Design

Selmihan Sahin*1 [ID]

Suleyman Demirel University, Arts and Science Faculty, Department of Chemistry, 32260, Isparta, Turkey

Abstract: In this study, TiO₂ nanoparticles were prepared and -COOH functionalized with 3-(3,4-dihydroxyphenyl) propionic acid. The characterization of nanoparticles was performed by FTIR, TEM, EDS and XRD. HRP was immobilized on those nanoparticles by EDC/NHS coupling reaction. The immobilization conditions of HRP including A: enzyme concentration (0.5-1.5 mg/mL), B: immobilization pH (4.0-8.0), C: immobilization temperature (4-50°C), D: immobilization time (1-20 h) were optimized by response surface methodology and Box-Behnken design. The optimized immobilization conditions were identified as 0.5 mg/mL HRP, at pH 5.5, 40 °C for 8 h for activity of immobilized HRP, 1.5 mg/mL HRP, at pH 4 and 18°C for 20 h for protein binding yield (%). At these optimum conditions, the experimental value for the activity of immobilized HRP was 80.39 U ± 1.06; protein binding yield was 94.25 ± 3.58%. Moreover, the optimum temperature and pH of free and immobilized enzyme were determined as 50°C and 4.0; 50°C and 3.5, respectively. The activity of the immobilized HRP sustained 52% of its initial activity after 10 days storage at 4°C. Furthermore, the immobilized HRP sustained 48% of its initial activity after 6 consecutive reactions.

Horseradish Peroksidaz Enziminin TiO₂-COOH Nanopartiküller Üzerine İmmobilizasyon Koşullarının Box-Behnken Metodu ile Optimize Edilmesi

Özet: Bu çalışmada, TiO₂ nanopartiküller hazırlandı ve 3-(3,4-dihidroksifenil) propiyonik asit ile –COOH fonksiyonelleştirildi. FTIR, TEM, EDS ve XRD ile nanopartiküllerin karakterizasyonu gerçekleştirildi. HRP elde edilen nanopartiküllerin üzerine EDC/NHS bağlama yolu ile immobilize edildi. A: enzim konsantrasyonu (0.5-1.5 mg/mL), B: immobilizasyon pH'sı (4.0-8.0), C: immobilizasyon sıcaklığı (4-50°C), D: immobilizasyon süresi (1-20 h)'ni içeren HRP'nin immobilizasyon koşulları yanıt yüzey yöntemi ve Box-Behnken dizayn kullanılarak optimize edildi. Optimize edilen immobilizasyon koşulları, immobilize HRP aktivitesi için 0.5 mg/mL HRP, pH 5.5, 40 °C ve 8 saat, protein bağlama verimi (%) için 1.5 mg/mL HRP, pH 4, 18°C ve 20 saat olarak belirlendi. Bu immobilizasyon koşullarında immobilize HRP için elde edilen deneysel değer 80.39 U ± 1.06 iken, protein bağlama verimi 94.25 ± 3.58%'dir. Bunun dışında serbest ve immobilize enzimin optimum sıcaklık ve pH değeri sırasıyla 50°C ve 4.0; 50°C ve 3.5 olarak belirlendi. 4°C'de 10 gün saklama sonunda immobilize HRP'nin başlangıç aktivitesinin %52'si kalmıştır. Ayrıca immobilize HRP 6 kez arka arakaya kullanım sonucunda başlangıç aktivitesinin %48'ini sürdürmüştür.

1. Introduction

Horseradish peroxidase (HRP) is an oxidoreductase (EC 1.11.1.7), which utilizes hydrogen peroxide to catalyze the oxidation of variety of organic and inorganic compounds [1]. It is one of the most studied enzymes, which has several applications in biotechnology [2] such as removal of phenols from

Corresponding author: selmihansahin@sdu.edu.tr

wastewater, organic synthesis and some biological applications (i.e. DNA sensors) [3-5]. Using soluble form of enzymes has some limitation for huge volume applications. However, immobilization of enzymes on solid support has several advantages such as enhanced stability, protection enzymes against denaturation and proteolysis, easy product recovery, reusability and contamination [6].

Natural polimers (alginate, agarose, chitin, chitosan etc.), synthetic polymers (polyvinyl alcohol, polyethylene glycol etc.) and inorganic materials (zeolites, celites, silica etc.) can be used as solid support materials for immobilization of enzymes [7]. Among these, inorganic support materials usually have high mechanical advantages, thermal stability and resistant to microbial action and organic solvents. Inorganic materials such as Au, SiO_2, Fe_3O_4 and TiO_2 have been used as a support for covalent immobilization of enzymes, so far. [8-10]. Among them, TiO_2 is quite special as a support because of its excellent resistance to pH and corrosion, superior mechanical strength, and outstanding antimicrobial performance [10,11]. Previously, HRP has been immobilized on colloidal Au modified ITO glass support [12], colloid/cysteamine-modified gold electrode [13], on Fe_3O_4/nanotubes composites by APTES [5], cubic mesoporous silicate (SBA-16) [14], modified acrylonitrile copolymer membrane [15], kaolin [16], mesoporous activated carbon [17], wool [18], chitosan crosslinked with cyanuric chloride [6], acrylic polymer activated by cyanuric chloride [19], bacterial cellulose [20], magnetic composite microsphere containing polyethylene glycol [21], multi-walled carbon nanotubes (MWCNTs) buckypaper/polyvinyl alcohol composite membrane[22].

To the best of our knowledge, however, there are no reports on the use of TiO_2 nanoparticles (TiNPs) as support material for HRP immobilization. However, the low amount of biomaterials is immobilized on the TiNPs because of their insufficient functional groups and inorganic structure. Surface modification is an effective mechanism to improve the biocompatibility of TiO_2, thus the amount of biomaterials immobilized on its surface can be increased [23]. Besides, it is generally needed to surface functionalization for covalent immobilization of enzymes on inorganic support materials [10]. For this reason, 3-(3,4-dihydroxyphenyl) propionic acid (3-DHPPA) was used for functionalization of TiNPs with –COOH group and then, HRP was immobilized on these nanoparticles through 1-ethyl-3-[3-dimethylaminopropyl] carbodiimide hydrochloride/N-hydroxysuccinimide (EDC/NHS) coupling reaction. Immobilization was verified by FTIR analysis and TEM, EDS and XRD analyses were used for characterization of TiNPs. RSM was used for evaluating the effects of various parameters (enzyme concentration, immobilization pH, temperature and time) and their interactions on immobilization of HRP through a small number of experiments. Furthermore, optimum pH and temperature, reusability and storage stability of immobilized HRP were determined.

2. Materials and methods

Peroxidase from horseradish lyophilized powder (~150 U/mg), EDC and NHS were purchased from Sigma-Aldrich. All other chemicals used were of analytical reagent grade.

2.1. Preparation of TiNPs

TiNPs were synthesized by using sol-gel method according to Wu et al., 2013 [10] with a minor modification, such as increasing of tetrabutoxytitanium (TBT) concentration with aim to obtain high amount of TiNPs. Briefly, 0.035 mole TBT (12 ml) was added into a three neck round bottom flask containing 100 mL of ethylene glycol and then, magnetically stirred for 20 h at 30°C under nitrogen atmosphere. After this, the obtained solution was transferred into acetone solution (final concentration: 0.077 M) containing ~0.3 wt.% of water under vigorous stirring for 30 min. The white precipitate occurred with aging about 1 h was collected by centrifugation and washed with water and ethanol to remove the residual ethylene glycol. TiNPs were dried at 80 °C for 24 h.

2.2. Carboxylation surface of TiNPs

The surface modification of the TiNPs was performed by using 3-DHPPA [10]. Firstly, 0.5 g the TiNPs were added into 3-DHPPA aqueous solution in pH 2.5 HCl (4 mg/mL) and then, vigorously stirred for 30 min. The modified nanoparticles were collected and washed with water and then dried at 50°C for 24 h. Carboxylated TiNPs were named as TiNPs-COOH.

2.3. Immobilization of HRP on TiNPs-COOH

HRP was immobilized on TiNPs-COOH by EDC/NHS coupling reaction. For EDC/NHS activation, 50 mg of TiNPs-COOH was dispersed in KH_2PO_4 buffer (50 mM, pH 6.0) by ultrasonication for 15 min. Then, 0.005 mol of EDC and NHS was added into the suspension and stirred at 130 rpm for 3 h. The activated TiNPs-COOH were washed with KH_2PO_4 buffer (50 mM, pH 6.0) and dried at 50 °C for 24 h.

HRP solution was prepared in proper buffer and then added onto 10 mg of the activated TiNPs-COOH. The covalent immobilization of HRP was performed at different time and temperature stirring at 110 rpm. The immobilized HRP (IHRP) were washed with proper buffer three times. In order to determine the protein binding yield, the residual enzyme amount in

the supernatant and initial enzyme amount were measured with Bradford method.

2.4. Characterization of support

2.4.1. FT-IR analyses

FT-IR spectra of TiO_2, TiNPs-COOH, EDC/NHS activated TiNPs-COOH nanoparticles and IHRP were recorded by FT-IR spectrometer.

2.4.2. TEM and EDS analyses

The morphology of TiNPs, TiNPs-COOH and EDC/NHS activated TiNPs-COOH nanoparticles was analyzed by TEM analysis. EDS was used to examine the elemental composition of the TiNPs and TiNPs-COOH.

2.4.3. XRD analyses

XRD analyses for TiNPs, TiNPs-COOH and EDC/NHS activated TiNPs-COOH were performed.

2.4.4. Activity assay

The activities of the free enzyme and IHRP were spectrophotometrically determined at 460 nm [15]. 0.1 mL of free enzyme or 10 mg of IHRP were added to the reaction mixture. The change of absorbance was determined at 460 nm for 1 min.

2.5. Influence of pH and temperature on free and immobilized enzyme

The influence of pH on the activities of free enzyme and IHRP was studied in different buffer with pH value from 3.0 to 9.0 (sodium acetate buffer 50 mM, pH 3.0–6.0; KH_2PO_4 buffer 50 mM, pH 6.0-8.0; Tris–HCl buffer 50 mM, pH 8.0-9.0) at room temperature.

The influence of temperature on the activities of free enzyme and IHRP were determined at different temperatures (30-70°C). The relative activity of the enzyme was calculated.

2.6. Reusability and storage stability

The reusability of the IHRP was determined by using it several times. After each activity assay, the IHRP were removed from reaction mixture and washed with acetate buffer (50 mM, pH 3.5). The next experiment was performed with fresh reaction mixture.

For determination of the storage stability of free enzyme and IHRP, they were kept at 4°C, and acetate buffer (50 mM, pH 3.5) and then, the activity of free enzyme and IHRP were determined under optimum conditions. After each assay the IHRP was removed from the reaction mixture and then, washed with

same buffer and kept at 4°C until next activity measurement.

The first measured activity was taken as control (100%) and the residual percentage of activity after each use was determined.

2.7. Experimental set up and statistical analysis

'Design Expert' software (V7 trial version, Stat-Ease Inc., Minneapolis, USA) was used for experimental design and analysis. Four independent variables were designed using Box-Behnken design (BBD) to determine optimum conditions for immobilization of HRP onto the EDC/NHS activated TiNPs-COOH. The used values for the optimization of immobilization conditions were decided with performing some preliminary experiments (data not shown). The influences of independent variables on the activity of the IHRP and protein binding yield (dependent variables) was investigated at three levels (+1, 0, and -1) by BBD (Table 1).

Table 1. Values of coded levels tested in BBD

Independent variables	Code units	Actual levels of coded factors		
		-1	0	1
Enzyme concentration	A	0.5	1	1.5
Immobilization pH	B	4.0	6.0	8.0
Immobilization temperature	C	4	27	50
Reaction time	D	1	10.5	20

A total of 29 experimental runs were designed and the center point was repeated five times to test the reproducibility of the test results.

3. Results and discussion

3.1. Characterization of support

3.1.1. FTIR analyses

FTIR spectra of bare TiNPs (a), TiNPs-COOH (b), EDC/NHS activated TiNPs-COOH (c), IHRP (d), HRP (e) are shown in Figure 1.
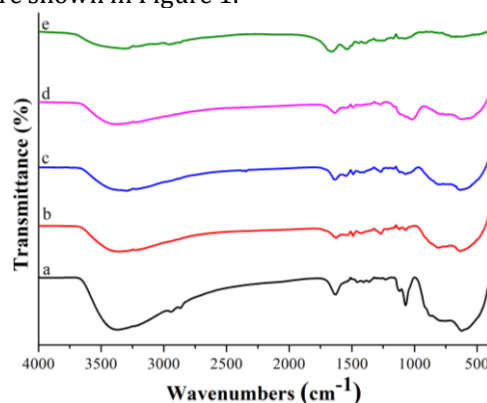
Figure 1. FTIR spectra of TiO_2 (a), TiNPs-COOH (b), EDC/NHS activated TiO_2-COOH (c), IHRP (d), HRP (e).
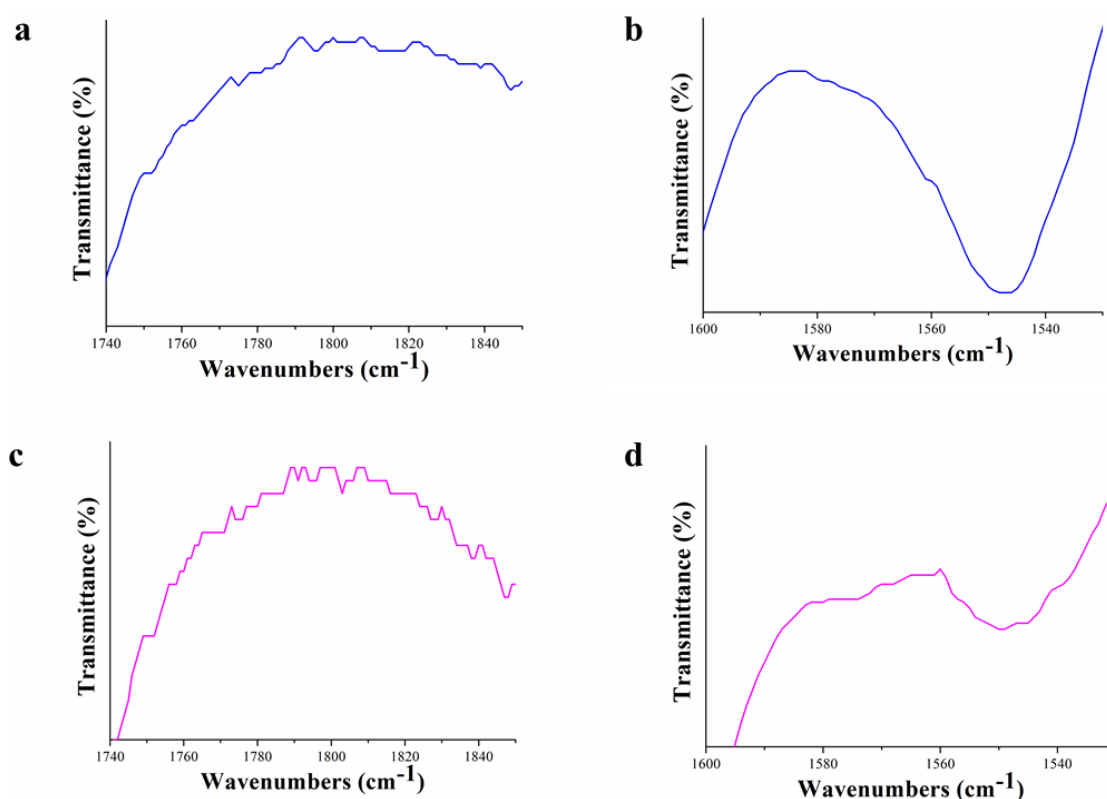
Figure 2. FTIR spectra of EDC/NHS activated TiNP-COOH (a, b) and IHRP (c, d).
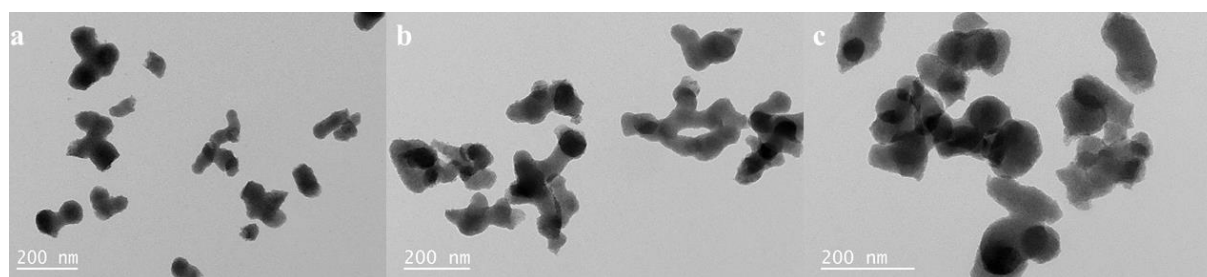
Figure 3. TEM image of TiNPs (a), TiNPs-COOH (b) and IHRP (c).

The spectra of a, b, c, d display a broad band in the range 600-700 cm^{-1} which is due to the vibration of Ti-O-Ti bond. In the spectrum of bare TiO₂ (a), the peak at 3370 cm^{-1} corresponds to –OH groups of weakly chemisorbed and physisorbed water [24]. Also, the absorption bands at 1073, 1223, 2864, 2930 cm^{-1} could be related with C-C-O- asymmetric stretch and symmetric and asymmetric –CH₂ stretching vibration of ethylene glycol, respectively. All these peaks vanished after –COOH functionalization [10]. For the –COOH functionalized TiNPs in Figure 5b, two new vibrational bands appear at 1486 cm^{-1} and at 1545 cm^{-1} assigned to the asymmetric stretching vibration of dissociated COO− groups, and carbonyl stretching vibration of the of -COOH groups (-C=O), respectively [10,25].

After EDC/NHS activation, appeared new peaks at 1770 and 1790 cm^{-1} were attributed to the carbonyl stretching vibration and NHS-ester, respectively (Figure 1c, 2a and 2c) [25].

As seen from Figure 1d and Appendix A, amide II band at 1574 cm^{-1} confirms the presence of enzyme on the support [10].

The FTIR analysis indicated that the synthesis of TiNPs, –COOH functionalization, activation with EDC/NHS reaction and immobilization of HRP on support were successfully performed.

3.1.2. TEM and EDS analyses

The size and morphology of TiNPs depend on the synthesis conditions. [26]. The size and shape of the obtained TiO₂ nanoparticles, TiO₂-COOH nanoparticles and immobilized HRP were studied by TEM (Figure 3). As a result of TEM analysis, it was obtained that all samples were dispersed and there was no any aggregation. The average particle size of them were measured in the range of 100-130 nm.

Synthesis of TiNPs and -COOH functionalization verified by EDS analyses (Figure 4).

907

The results are presented in Table 2. The 'Ti' and 'O' elements were obviously found in both EDS spectra. All results indicated that TiNPs were successfully prepared without any contamination. Also, increased atomic weight of 'O' showed that carboxylation of TiNPs (–COOH) was successfully performed.

Table 2. The element compositions of TiNPs and TiNPs-COOH from EDS analysis (atomic wt.%).

	Ti	O	C
TiNPs	40.2	25.7	34.1
TiNPs-COOH	25.9	42.8	31.3
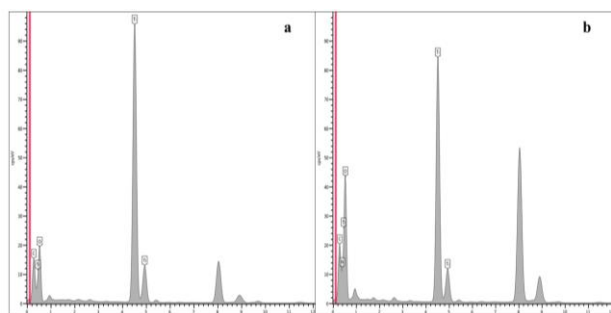
Figure 4. EDS analyses of TiNPs (a) and TiNPs-COOH.

3.1.3. XRD analyses

Figure 5 shows the XRD patterns for TiNPs and TiNPs-COOH. Both samples don't have any diffraction peak. It can be suggested that the obtained nanoparticles have amorphous structure. The obtained results are in accordance with previous reports by Pal et al.[26].
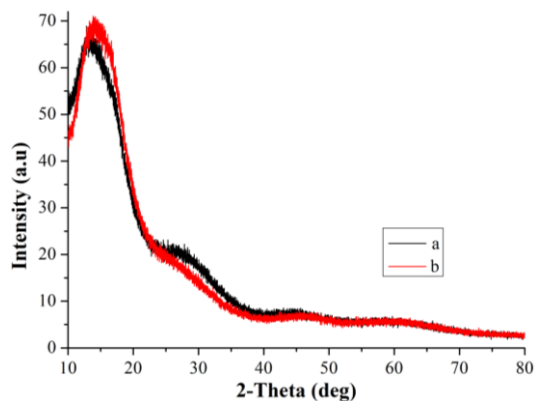
Figure 5. XRD patterns of TiNPs (a) and TiNPs-COOH (b).

3.2. Immobilization of HRP on TiNPs-COOH

The optimization of each immobilization parameters one by one needs intensive working and extensive time. But, the effects of various parameters on response can be evaluated with RSM by reducing the number of experiments [27]. For this reason, RSM was used to investigate the influence of parameters (A, B, C, D) on the activity of IHRP and protein binding yield onto the EDC/NHS activated TiNPs-COOH and results were presented in Table 3.

To find the suitable model for the formation of regression equation of the experimental data, different statistical models such as linear, 2F1, quadratic and cubic were analyzed (CV%=15.74). Regression equation provides the level of the activity of IHRP and protein binding yield as a function of different variables by means of ANOVA.
Following equations include all the terms:

$$IHRP_{activity} = \begin{Bmatrix} +74.37 - 0.59A - 5.22B \\ +2.03C - 6.96D + 3.38AB \\ -16.58AC + 2.73AD - 6.87BC \\ -4.89BD - 2.28CD - 1.33A^2 \\ -22.46B^2 - 18.40C^2 - 18.33D^2 \end{Bmatrix} \quad (1)$$

$$Protein_{binding} = \begin{Bmatrix} +37.54 + 3.31A - 20.56B \\ +13.83C + 23.40D - 0.92AB \\ +2.98AC + 12.12AD - 8.98BC \\ -18.42BD + 8.35CD - 2.80A^2 \\ -10.61B^2 - 1.00C^2 + 8.49D^2 \end{Bmatrix} \quad (2)$$

As seen in Table 4, p>F<0.0500 indicated that quadratic regression surface model was statistically significant to represent of the activity of IHRP (F-value of 21.65 and p-value of <0.0001) and protein binding yield (F-value of 1297.85 and p-value of <0.0001).

This model was suitable model owing to high F-values evaluated by using sequential sum of squares and ANOVA. The coefficient of variance [28] values (10.64 for the activity of IHRP, 16.55 for the protein binding yield) indicated the precision and reliability [29].

The lack of fit was not significant for the activity of IHRP and protein binding yield. Thus, the model has ability to predict the activity of IHRP and protein binding yield within a range of variable values. If the coefficient of value (R^2) is the closer is to 1.00, it can be obtained better results to predict the response with the model [27]. The R^2 values were evaluated as 0.9558 for the activity of the IHRP, 0.9747 for the protein binding yield with fitted model; those were in reasonably close with the R_{adj}^2 of 0.9117 and 0.9493, respectively. The difference between R^2 and R_{adj}^2 is <0.2 suggesting that sample range is adequately large [29,30].

Additionally, the results indicated that B and D were the single parameters affecting the activity of IHRP, whereas B, C and D parameters had significant effect on the protein binding yield (Table 4).

Contour plots of the activity of IHRP are presented in Figure 6. The influences of enzyme concentration and immobilization pH on the activity of IHRP at the immobilization temperature (27°C) and immobilization time (10.5 h) are illustrated in Figure 6a. It was found that the immobilization pH had a more important effect on the activity of IHRP than the enzyme concentration. Also, the interaction between enzyme concentration and

immobilization pH was not statistically significant ($p>0.05$).

Table 3. Experimental design based on BBD and experimental results of the HRP immobilization on TiNPs-COOH by EDC/NHS activation.

Run	Variable level				Activity of IHRP[a]		Protein binding yield (%)	
	A	B	C	D	Determined	Predicted	Determined	Predicted
1	0.50	4.00	27.00	10.50	60.97	59.78	45.16	40.47
2	1.50	4.00	27.00	10.50	53.45	51.83	48.90	48.92
3	0.50	8.00	27.00	10.50	42.03	42.57	3.8	1.18
4	1.50	8.00	27.00	10.50	48.05	48.17	3.87	5.97
5	1.00	6.00	4.00	1.00	44.69	40.29	12.29	16.15
6	1.00	6.00	50.00	1.00	53.84	48.91	30.59	27.12
7	1.00	6.00	4.00	20.00	27.07	30.93	45.37	46.24
8	1.00	6.00	50.00	20.00	27.11	30.44	97.08	90.61
9	0.50	6.00	27.00	1.00	59.06	64.98	25.71	28.65
10	1.50	6.00	27.00	1.00	52.40	58.36	12.62	11.02
11	0.50	6.00	27.00	20.00	45.48	45.62	49.26	51.19
12	1.50	6.00	27.00	20.00	49.73	49.90	84.66	82.06
13	1.00	4.00	4.00	10.50	27.09	29.82	25.11	23.68
14	1.00	8.00	4.00	10.50	31.06	33.14	4.47	0.52
15	1.00	4.00	50.00	10.50	43.62	47.64	65.03	69.31
16	1.00	8.00	50.00	10.50	20.09	23.46	8.47	10.23
17	0.50	6.00	4.00	10.50	38.93	36.62	19.16	19.58
18	1.50	6.00	4.00	10.50	70.53	68.60	19.99	20.23
19	0.50	6.00	50.00	10.50	76.92	73.84	39.22	41.28
20	1.50	6.00	50.00	10.50	42.20	39.51	52	53.87
21	1.00	4.00	27.00	1.00	41.59	40.87	15.24	14.16
22	1.00	8.00	27.00	1.00	42.03	40.22	10.52	9.89
23	1.00	4.00	27.00	20.00	39.92	36.74	94.88	97.81
24	1.00	8.00	27.00	20.00	20.80	16.52	16.47	19.83
25	1.00	6.00	27.00	10.50	75.84	74.37	46.49	37.54
26	1.00	6.00	27.00	10.50	73.53	74.37	42.27	37.54
27	1.00	6.00	27.00	10.50	65.05	74.37	37.83	37.54
28	1.00	6.00	27.00	10.50	75.84	74.37	24.26	37.54
29	1.00	6.00	27.00	10.50	81.59	74.37	36.86	37.54

[a]U/g support

Table 4. The variance analysis of response factor based on the activity of IHRP and protein binding yield

	Activity of IHRP			Protein binding yield		
	Degree of freedom	F value	$p>F$	Degree of freedom	F value	$p>F$
Model	14	21.65	<0.0001*	14	38.47	<0.0001*
A-Enyzme Concentration	1	0.15	0.7047	1	3.90	0.0684
B-Immobilization pH	1	11.84	0.0040*	1	150.38	<0.0001*
C-Immobilization Temperature	1	1.80	0.2009	1	68.07	< 0.0001*
D-Immobilization Time	1	21.07	0.0004*	1	194.70	< 0.0001*
AB	1	1.66	0.2181	1	0.100	0.7571
AC	1	39.89	< 0.0001*	1	1.06	0.3216
AD	1	1.08	0.3167	1	17.43	0.0009*
BC	1	6.86	0.0202*	1	9.56	0.0079*
BD	1	3.47	0.0835	1	40.25	<0.0001*
CD	1	0.75	0.3999	1	8.27	0.0122*
A²	1	0.41	0.5299	1	1.51	0.2392
B²	1	118.71	< 0.0001*	1	21.63	0.0004*
C²	1	79.71	< 0.0001*	1	0.19	0.6676
D²	1	79.09	< 0.0001*	1	13.85	0.0023*
Residual	14			14		
Lack of Fit	10	0.67	0.7228	10	0.28	0.9550
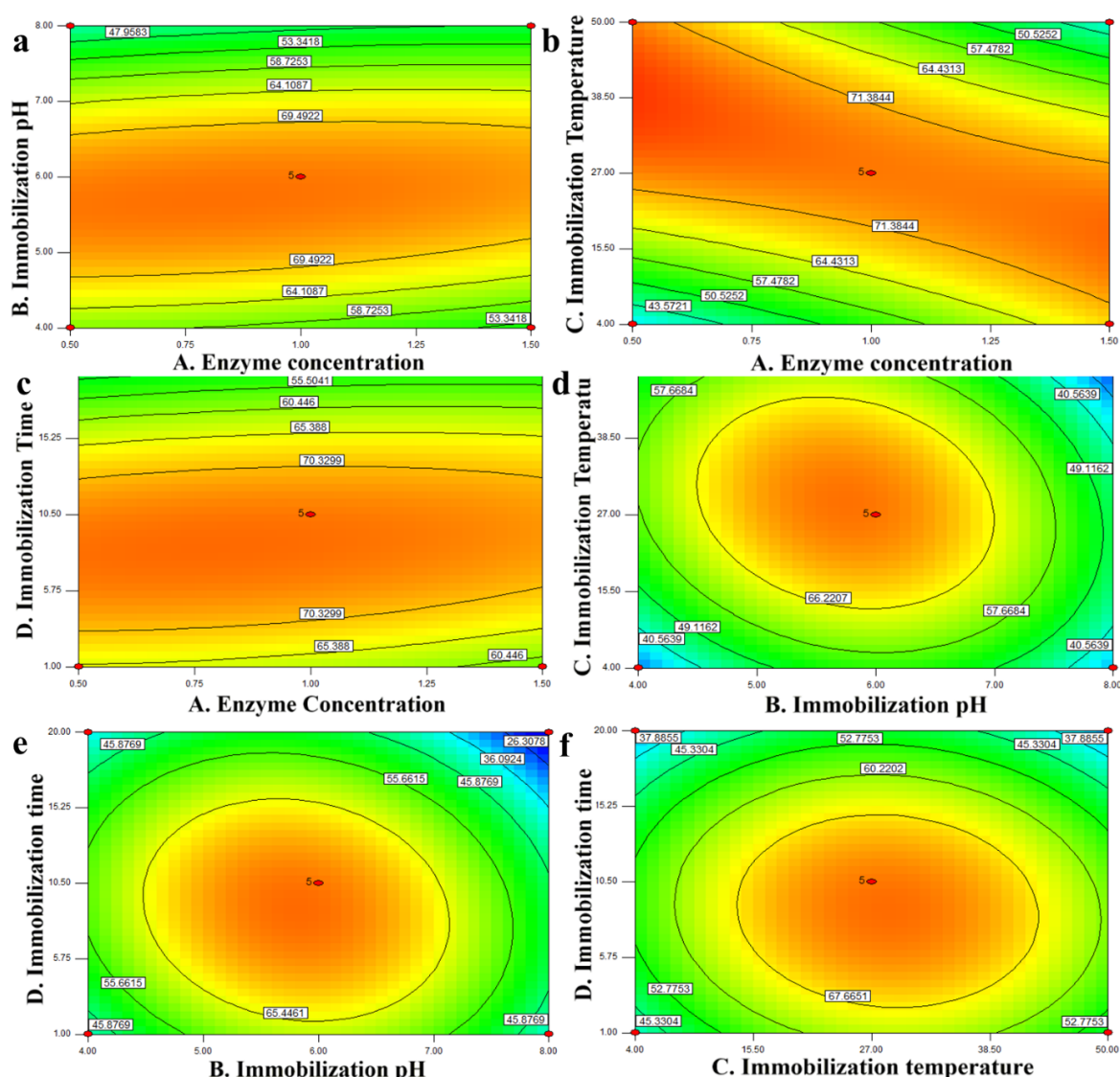
Figure 6. Contour plots display the influence of immobilization conditions on the activity of IHRP on the TiNPs-COOH. Effect of (a) enzyme concentration and immobilization pH, (b) enzyme concentration and immobilization temperature, (c) enzyme concentration and immobilization time, (d) immobilization pH and temperature, (e) immobilization pH and time, (f) immobilization temperature and time.

Figure 6b demonstrates the influence of enzyme concentration and immobilization temperature on the activity of IHRP under the immobilization conditions of pH 6.0 and 10.5 h. Also, interaction between enzyme concentration and immobilization temperature was significant ($p<0.05$). The IHRP activity increased with the increased concentration of enzyme at low temperature, while it decreased at high temperature.

Figure 6c presents the influence of enzyme concentration and immobilization time on the activity of IHRP at the 27°C and pH 6.0. When the concentration of HRP solution was fixed at a point, the IHRP activity initially increased, then decreased with the time.

Figure 6d demonstrates the influence of immobilization pH and immobilization temperature on the IHRP at the enzyme concentration of 1 mg/mL and immobilization time of 10.5 h with hyperbolic behavior. The interaction between enzyme concentration and immobilization pH was significant ($p<0.0202$). A maximum activity of IHRP was obtained at pH 6.0 and 27°C.

The influence of immobilization pH and time on the activity of IHRP at the 27°C and 1 mg/mL of the enzyme concentration are shown in Figure 6e. Although the IHRP activity was maximum at pH 6.0 and 10.5 h, it was increased with time, and then decreased at pH 6.0. Also, the interaction between enzyme concentration and immobilization pH was not significant ($p>0.0835$).

Figure 6f presents the influence of temperature and time on the activity of IHRP at the pH 6.0 and enzyme concentration of 1 mg/mL. The interaction between temperature and pH wasn't significant ($p>0.05$).

Figure 7a demonstrates the influence of enzyme concentration and immobilization pH on protein

binding yield. When the enzyme concentration was set at the mid-point (0:1 mg/mL) and immobilization pH was at the +1 point (8.0), the interaction between enzyme concentration and immobilization pH wasn't significant (p>0.05). Protein binding yield was decreased with increased pH, while there is no effect of enzyme concentration on the protein binding yield.

Figure 7b presents the contour plot of enzyme concentration and immobilization temperature at the 0, +1 points. Immobilization temperature has a stronger effect on the protein binding yield than the enzyme concentration. When the enzyme concentration was maximum, the protein binding yield was increased with immobilization temperature higher than 27°C.

In Figure 7c presents the influence of enzyme concentration and immobilization time on the protein binding yield at 27°C and pH 6.0. The interaction between enzyme concentration and immobilization time was significant ($p<0.05$). As enzyme concentration was increased, protein binding yield became maximum with increased immobilization time.

Looking at Figure 7d, enzyme concentration and immobilization time were kept at the center points of 1 mg/mL and 10.5 h (0, 0). At immobilization pH lower than 6.0, protein binding yield increased with the increased immobilization temperature.

Figure 7e shows the influence of the immobilization pH and time on the protein binding yield under the 27°C of immobilization conditions and 1 mg/mL of enzyme concentration. The interaction between the immobilization pH and time was significant ($p<0.05$). Protein binding yield was optimum at pH 4.0-5.0 and with increased immobilization time.

Figure 7f illustrates the influence of immobilization temperature and time on the protein binding yield values at the enzyme concentration of 1 mg/mL and pH 6.0. The interaction between the immobilization pH and time was significant ($p<0.05$). The protein binding yield was increased with increased immobilization temperature and time.

Sulfo-NHS has very low pKa value thus, surface of EDC/NHS activated TiNPs-COOH can be negatively charged broad pH range [31]. Besides, HRP has positive net charge below pH 8.0 (pI~8.9) [32]. Amine residues are highly deprotonated around pH 7.0 value, which results in increased binding yield of protein. Also, the reactivity of NHS esters towards amine groups is decreased below pH 5.0 [33]. According to the results, protein binding yield was maximum at pH 4.0. It could be attributed that HRP immobilized on the EDC/NHS activated TiNPs-COOH by electrostatic interactions below pH 5.0. However, the IHRP activity was maximum at pH 6.0. The absorption of protein onto the support surfaces causes protein denaturation and

conformational changes result in losses of activity. Also, crowded surface of the support may cause the reduced activity due to diffusional limitations [34]. All these reasons can be explained the decrease of the IHRP activity as the protein binding yield increased.

Kazanwedel et al. [35] similarly obtained that immobilization of HRP on functionalized magnetic nanoparticle by EDC result in optimum protein binding yield at pH 4.0. But, HRP immobilized at pH 5.3 showed the highest activity. Likewise, they also recommended that immobilization at pH 7.0 was not ideal in terms of protein binding and activity of IHRP [35].

Immobilization of HRP onto kaolin provided maximum activity at pH 5.0, while the activity of IHRP at above pH 7.0 was significantly reduced [16]. Temperature is also an important parameter for immobilization. As the temperature increased the higher protein binding yield values were obtained. It can be attributed that increased thermal vibration of enzyme and support with temperature lead to increasing enzyme binding on the support [30],[36]. Otherwise, the activity of IHRP decreased with increased temperature. This could be related with denaturation of enzyme with temperature [22].

It could be seen from to the results, the IHRP showed optimum activity after immobilization for 10.5 h and the activity of IHRP was diminised with further immobilization time while protein binding yield increased further prolonged immobilization time. It can be said that HRP can't complete contact with support with short time immobilization. Although enzyme can effectively bind on the support with extended time, it can be partially inactivated with time and excessive immobilization of HRP on the support can cause substrate diffusion limitations or conformational change [30,37].

3.3. Optimization and validation of immobilization conditions

The optimization of parameters for the immobilization of HRP were performed by using the Box-Benhken model according to the highest activity and protein binding yield. From the predicted optimum conditions, the validation of the model was performed with triplicate experiments. The activity of IHRP was predicted as 81.2847 U/g when immobilization was performed with 0.5 mg/mL HRP, at pH 5.5, 40 °C for 8 h. The protein binding yield was predicted as 97.063% when immobilization was performed with 1.5 mg/mL HRP, at pH 4.0 and 18°C for 20 h. The experimental value for activity of IHRP was 80.39 ± 1.06 U/g, protein binding yield was 94.25 ± 3.58%. The results were very close to the predicted value by the model, within 95% confidence level.
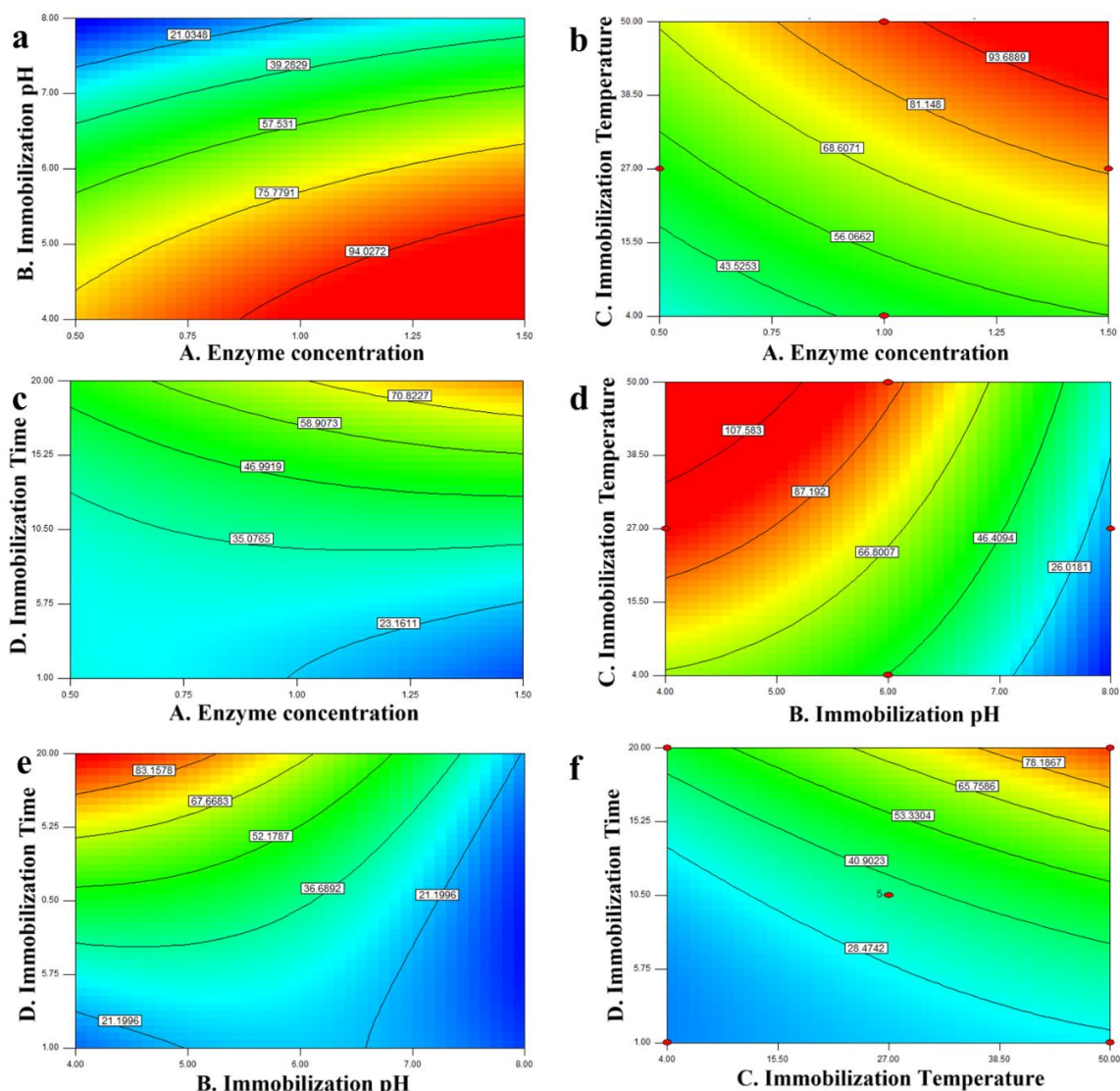
Figure 7. Contour plots display the influence of immobilization conditions on the protein binding yield on the TiNPs-COOH. Effect of (a) enzyme concentration and immobilization pH, (b) enzyme concentration and immobilization temperature, (c) enzyme concentration and immobilization time, (d) immobilization pH and temperature, (e) immobilization pH and time, (f) immobilization temperature and time.

3.4. Optimum pH of free and immobilized enzyme

The influence of pH on the free enzyme and IHRP activity was studied at different pH values (3.0 to 9.0) at 25 °C. The effect of pH on the activity of the free enzyme and IHRP was demonstrated in Figure 8.
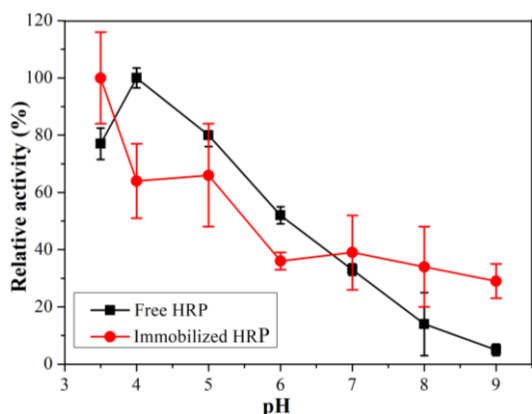
Figure 8. The effect of pH on the free enzyme and IHRP.

The free enzyme and IHRP displayed different behaviors depend on the pH. The optimum pH of the IHRP activity was at pH 3.5 when using acetate buffer (50 mM), whereas free enzyme showed optimum activity at pH 4.0 of acetate buffer (50 mM). After immobilization the optimum pH value of the HRP shifted 0.5 unit to the acidic region when compared with free one. Previously, similar results were reported by Mohamed et al.[6] shifting pH of HRP from 5.5 to 5.0 and by Jamal et al. [38] shifting pH of gourd peroxidase from 5.0 to 4.0 after immobilization. Both ionizable groups of enzymes and the characteristic properties of the support affects the optimum pH of the enzyme. Because of this, it can be said that pH is effective on the interaction between enzyme-support and the ionizable groups of enzyme Sahin and Ozmen [39]. Gao et al. [40] were indicated that HRP showed optimum activity at pH 4.0.

The optimum temperature of free enzyme and IHRP at optimum pH value was studied ranging from 30 °C to 70 °C. The effect of temperature on the activity of free enzyme and IHRP was demonstrated in Figure 9.

Although the optimum temperature for the free enzyme and the IHRP was identical and determined as 50°C, the IHRP showed higher residual activity at above that temperature. Immobilization of HRP on TiNPs-COOH by EDC/NHS activation increased the stability of enzyme and thus, the immobilized enzyme could retain more active than free one at higher temperature. This result is consistent with results of Yu et al.[20], Monier et al.[4], Mohamed et al.[6], El-Nahass et al. [14].
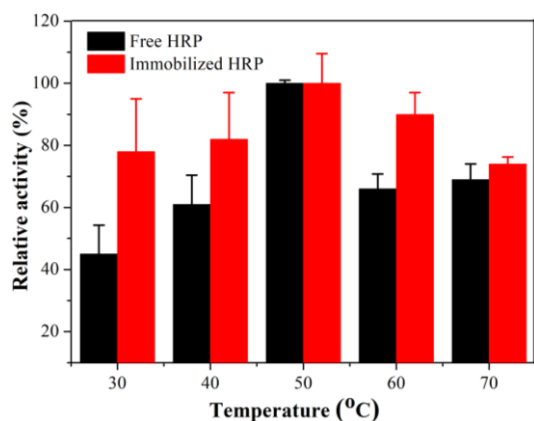
Figure 9. The effect of temperature on the free enzyme and IHRP.

3.5. Reusability

The reusability of immobilized enzyme was explored, and the results were given in Figure 10.
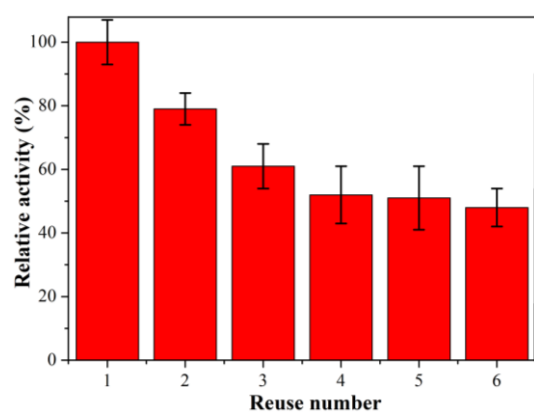
Figure 10. Reusability of the IHRP.

After 6 consecutive reactions, the IHRP sustained 48% of initial activity. Previously, IHRPs on different supports showed above fifty percent of initial enzyme activity after five [41], six [4,5] or ten cycles [14]. The reuse number of immobilized enzymes was related with support material and the substrate of the enzyme. The obtained decrease at the initial activity could be mainly assigned to the increased

concentration of the reaction products along with the reaction [41].

3.6. Storage stability

The storage stability of the free and IHRP (stored in 50 mM acetate buffer, at 4°C) was determined by measuring the activities at regular intervals. The results showed that the storage stability of the HRP was developed with immobilization on TiNPs-COOH (Figure 11).
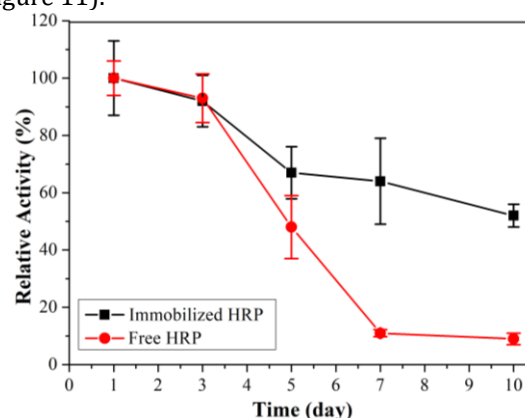
Figure 11. The storage stability of the free enzyme and IHRP.

The IHRP could still sustain 52% of its initial activity, while the free enzyme could sustain 9% of the initial activity after 10 days. According to these results, the immobilization of HRP on TiNPs-COOH by EDS/NHS activation seems to be advantageous in terms of stability. It could be said that, the immobilization protected enzyme against denaturation and thus, improved the storage stability of enzyme.

4. Conclusions

TiNPs were prepared and functionalized with 3-DHPPA successfully and then used for the HRP immobilization on the surface through EDC/NHS activation. FTIR, TEM, EDS and XRD analyses were used for the characterization of the TiNPs and verification of the immobilization. Influence of tested parameters on the response (activity of IHRP and protein binding yield) were determined and immobilization of HRP were statistically optimized to obtain maximum results by BBD. Quadratic model was fitted model for the results of the immobilized enzyme activity (F-value of 21.65 and *p*-value of <0.0001) and protein binding yield (F-value of 1297.85 and *p*-value of <.0001). CV values (10.64 for the activity of IHRP, 16.55 for the protein binding yield) indicated the precision and reliability. Based on the model, the optimum conditions for immobilization were predicted as 0.5 mg/mL HRP, at pH 5.5, 40°C for 8 h for activity of IHRP, 1.5 mg/mL HRP, at pH 4 and 18°C for 20 h for protein binding yield (%). The experimental value for activity of IHRP was 80.39 ± 1.06 (predicted: 81.2847 U), protein

binding yield was 94.25 ± 3.58% (predicted: 97.063%) at the optimum conditions. These results showed that BBD is a very effective tool for optimization of immobilization conditions. After that the optimum temperature and pH of the free and immobilized enzyme were determined. The optimum temperature of free enzyme and the IHRP was identical and at 50°C. The optimum pH for free enzyme was 4.0 that was higher than that of the IHRP (pH 3.5). The IHRP could still sustain 52% of its initial activity, whilst the free one could sustain 9% of the initial activity after 10 days. Furthermore, the IHRP showed 48% of its initial activity after 6 consecutive reactions. These results showed that the TiNPs-COOH could be promising support material for HRP. IHRP on TiNPs-COOH could have potential in various biotechnological, environmental and large scale industrial applications such as wastewater treatments, especially removing of phenol, drug delivery systems, biofuel cells and biosensors. .

References

[1] Shivakumar, A., Bg, J., Mr, D., 2017. Role of Peroxidase in Clinical Assays: A Short Review. Journal of Clinical Nutrition & Dietetics, 03.

[2] Lopes, G. R., Pinto, D. C. G. A., Silva, A. M. S., 2014. Horseradish peroxidase (HRP) as a tool in green chemistry. RSC Advances, 4. 37244-37265.

[3] Mohammed, L., Gomaa, H. G., Ragab, D., Zhu, J., 2017. Magnetic nanoparticles for environmental and biomedical applications: A review. Particuology, 30. 1-14.

[4] Monier, M., Ayad, D. M., Wei, Y., Sarhan, A. A., 2010. Immobilization of horseradish peroxidase on modified chitosan beads. International Journal of Biological Macromolecules, 46. 324-330.

[5] Zhang, C., Cai, X., 2018. Immobilization of horseradish peroxidase on Fe3O4/nanotubes composites for Biocatalysis-degradation of phenol. Composite Interfaces, 26. 379-396.

[6] Mohamed, S. A., Al-Malki, A. L., Kumosani, T. A., El-Shishtawy, R. M., 2013. Horseradish peroxidase and chitosan: activation, immobilization and comparative results. International Journal of Biological Macromolecules, 60. 295-300.

[7] Datta, S., Christena, L. R., Rajaram, Y. R., 2013. Enzyme immobilization: an overview on techniques and support materials. 3 Biotech, 3. 1-9.

[8] Aslani, E., Abri, A., Pazhang, M., 2018. Immobilization of trypsin onto Fe3O4@SiO2 - NH2 and study of its activity and stability. Colloids Surf B Biointerfaces, 170. 553-562.

[9] Libertino, S., Scandurra, A., Aiello, V., Giannazzo, F., Sinatra, F., Renis, M., Fichera, M., 2007. Layer uniformity in glucose oxidase immobilization on SiO2 surfaces. Applied Surface Science, 253. 9116-9123.

[10] Wu, H., Liang, Y., Shi, J., Wang, X., Yang, D., Jiang, Z., 2013. Enhanced stability of catalase covalently immobilized on functionalized titania submicrospheres. Materials Science and Engineering C, 33. 1438-1445.

[11] Carp, O., 2004. Photoinduced reactivity of titanium dioxide. Progress in Solid State Chemistry, 32. 33-177.

[12] Wang, L., 2004. A novel hydrogen peroxide sensor based on horseradish peroxidase immobilized on colloidal Au modified ITO electrode. Electrochemistry Communications, 6. 225-229.

[13] Yi, X., Huang-Xian, J., Hong-Yuan, C., 2000. Direct electrochemistry of horseradish peroxidase immobilized on a colloid/cysteamine-modified gold electrode. Analytical Biochemistry, 278. 22-28.

[14] El-Nahass, M. N., El-Keiy, M. M., Ali, E. M. M., 2018. Immobilization of horseradish peroxidase into cubic mesoporous silicate, SBA-16 with high activity and enhanced stability. Int J Biol Macromol, 116. 1304-1309.

[15] Vasileva, N., Godjevargova, T., Ivanova, D., Gabrovska, K., 2009. Application of immobilized horseradish peroxidase onto modified acrylonitrile copolymer membrane in removing of phenol from water. International Journal of Biological Macromolecules, 44. 190-194.

[16] Sekuljica, N. Z., Prlainovic, N. Z., Jovanovic, J. R., Stefanovic, A. B., Djokic, V. R., Mijin, D. Z., Knezevic-Jugovic, Z. D., 2016. Immobilization of horseradish peroxidase onto kaolin. Bioprocess and Biosystems Engineering, 39. 461-472.

[17] Jain, A., Ong, V., Jayaraman, S., Balasubramanian, R., Srinivasan, M. P., 2016. Supercritical fluid immobilization of horseradish peroxidase on high surface area mesoporous activated carbon. The Journal of Supercritical Fluids, 107. 513-518.

[18] Mohamed, S. A., Darwish, A. A., El-Shishtawy, R. M., 2013. Immobilization of horseradish peroxidase on activated wool. Process Biochemistry, 48. 649-655.

[19] Mohamed, S. A., Al-Ghamdi, S. S., El-Shishtawy, R. M., 2016. Immobilization of horseradish peroxidase on amidoximated acrylic polymer activated by cyanuric chloride. International Journal of Biological Macromolecules, 91. 663-670.

[20] Yu, B., Cheng, H., Zhuang, W., Zhu, C., Wu, J., Niu, H., Liu, D., Chen, Y., Ying, H., 2019. Stability and repeatability improvement of horseradish peroxidase by immobilization on amino-functionalized bacterial cellulose. Process biochemistry, 79, 40-48.

[21] Xie, X., Luo, P., Han, J., Chen, T., Wang, Y., Cai, Y., Liu, Q., 2019. Horseradish peroxidase immobilized on the magnetic composite microspheres for high catalytic ability and operational stability. Enzyme Microb Technol, 122. 26-35.

[22] Jun, L. Y., Mubarak, N. M., Yon, L. S., Bing, C. H., Khalid, M., Jagadish, P., Abdullah, E. C., 2019. Immobilization of Peroxidase on Functionalized MWCNTs-Buckypaper/Polyvinyl alcohol Nanocomposite Membrane. Scientific Reports, 9. 2215.

[23] Wu, L., Wu, S., Xu, Z., Qiu, Y., Li, S., Xu, H., 2016. Modified nanoporous titanium dioxide as a novel carrier for enzyme immobilization. Biosensors and Bioelectronic, 80. 59-66.

[24] Kumar, P. M., Badrinarayanan, S., Sastry, M., 2000. Nanocrystalline TiO2 studied by optical, FTIR and X-ray photoelectron spectroscopy: correlation to presence of surface states. Thin Solid Films, 358. 122-130.

[25] Psarra, E., König, U., Müller, M., Bittrich, E., Eichhorn, K.J., Welzel, P.B., Stamm, M., Uhlmann, P., 2017. In situ monitoring of linear RGD-peptide bioconjugation with nanoscale polymer brushes. ACS Omega, 2(3), 946-958.

[26] Pal, M., Serrano, J. G., Santiago, P., U., P., 2007. Size-Controlled Synthesis of Spherical TiO2 Nanoparticles: Morphology, Crystallization, and Phase Transition. The Journal of Physical Chemistry B, 111. 96-102.

[27] Hill, A., Karboune, S., Mateo, C., 2017. Investigating and optimizing the immobilization of levansucrase for increased transfructosylation activity and thermal stability. Process Biochemistry, 61. 63-72.

[28] Katz, E., MacVittie, K., 2013. Implanted biofuel cells operating in vivo – methods, applications and perspectives – feature article. Energy & Environmental Science, 6. 2791.

[29] Kamble, P. P., Kore, M. V., Patil, S. A., Jadhav, J. P., Attar, Y. C., 2018. Statistical optimization of process parameters for inulinase production from Tithonia weed by Arthrobacter mysorens strain no.1. Journal of Microbiological Methods, 149. 55-66.

[30] Dai, X. Y., Kong, L. M., Wang, X. L., Zhu, Q., Chen, K., Zhou, T., 2018. Preparation, characterization and catalytic behavior of pectinase covalently immobilized onto sodium alginate/graphene oxide composite beads. Food Chemistry, 253. 185-193.

[31] Pei, Z., Anderson, H., Myrskog, A., Duner, G., Ingemarsson, B., Aastrup, T., 2010. Optimizing immobilization on two-dimensional carboxyl surface: pH dependence of antibody orientation and antigen binding capacity. Analytical Biochemistry, 398. 161-168.

[32] Chouyyok, W., Panpranot, J., Thanachayanant, C., Prichanont, S., 2009. Effects of pH and pore characters of mesoporous silicas on horseradish peroxidase immobilization. Journal of Molecular Catalysis B: Enzymatic, 56. 246-252.

[33] Risse, F., Gedig, E. T., Gutmann, J. S., 2018. Carbodiimide-mediated immobilization of acidic biomolecules on reversed-charge zwitterionic sensor chip surfaces. Analytical and Bioanalytical Chemistry, 410. 4109-4122.

[34] Homaei, A. A., Sariri, R., Vianello, F., Stevanato, R., 2013. Enzyme immobilization: an update. Journal of Chemical Biology, 6. 185-205.

[35] Kazenwadel, F., Wagner, H., Rapp, B. E., Franzreb, M., 2015. Optimization of enzyme immobilization on magnetic microparticles using 1-ethyl-3-(3-dimethylaminopropyl) carbodiimide (EDC) as a crosslinking agent. Analytical Methods, 7. 10291-10298.

[36] Fernández-Lorente, G., Lopez-Gallego, F., Bolivar, J., Rocha-Martin, J., Moreno-Perez, S., Guisan, J., 2015. Immobilization of Proteins on Highly Activated Glyoxyl Supports: Dramatic Increase of the Enzyme Stability Multipoint Immobilization on Pre-existing Carriers. Current Organic Chemistry, 19. 1719-1731.

[37] Al-Dhrub, A. H. A., Sahin, S., Ozmen, I., Tunca, E., Bulbul, M., 2017. Immobilization and characterization of human carbonic anhydrase I on amine functionalized magnetic nanoparticles. Process Biochemistry, 57. 95-104.

[38] Jamal, F., Qidwai, T., Singh, D., Pandey, P. K., 2012. Biocatalytic activity of immobilized pointed gourd (Trichosanthes dioica) peroxidase–concanavalin A complex on calcium alginate pectin gel. Journal of Molecular Catalysis B: Enzymatic, 74. 125-131.

[39] Sahin, S., Ozmen, I., 2016. Determination of optimum conditions for glucose-6-phosphate dehydrogenase immobilization on chitosan-coated magnetic nanoparticles and its characterization. Journal of Molecular Catalysis B: Enzymatic, 133. S25-S33.

[40] Gao, L., Zhuang, J., Nie, L., Zhang, J., Zhang, Y., Gu, N., Wang, T., Feng, J., Yang, D., Perrett, S., Yan, X., 2007. Intrinsic peroxidase-like activity of ferromagnetic nanoparticles. Nature nanotechnology, 2(9), 577.

[41] Zhai, R., Zhang, B., Wan, Y., Li, C., Wang, J., Liu, J., 2013. Chitosan–halloysite hybrid-nanotubes: Horseradish peroxidase immobilization and applications in phenol removal. Chemical Engineering Journal, 214. 304-309.